

Dysfunctional subsets of CD39⁺ T cells, distinct from PD-1⁺, driven by leukemic extracellular vesicles in myeloid leukemias

Julian Swatler,^{1,2} Domenico Lo Tartaro,² Rebecca Borella,² Marta Brewinska-Olchowik,¹ Annamaria Paolini,² Anita Neroni,² Laura Turos-Korgul,¹ Milena Wiech,¹ Ewa Kozłowska,³ Dominik Cysewski,^{4,°} Wioleta Grabowska-Pyrzewicz,⁵ Urszula Wojda,⁵ Grzegorz Basak,⁶ Rafael J. Argüello,⁷ Andrea Cossarizza,^{2,8} Sara De Biasi^{2#} and Katarzyna Piwocka^{1#}

¹Laboratory of Cytometry, Nencki Institute of Experimental Biology, Warsaw, Poland; ²Department of Medical and Surgical Sciences for Children & Adults, University of Modena and Reggio Emilia, Modena, Italy; ³Department of Immunology, Faculty of Biology, University of Warsaw, Warsaw, Poland; ⁴Laboratory of Mass Spectrometry, Institute of Biochemistry and Biophysics, Warsaw, Poland; ⁵Laboratory of Preclinical Testing of Higher Standard, Nencki Institute of Experimental Biology, Warsaw, Poland; ⁶Department of Hematology, Transplantation and Internal Medicine, Medical University of Warsaw, Warsaw, Poland; ⁷Aix Marseille University, CNRS, INSERM, CIML, Centre d'Immunologie de Marseille-Luminy, Marseille, France and ⁸National Institute for Cardiovascular Research, Bologna, Italy

[°]Current address: Clinical Research Center, Medical University of Białystok, Białystok, Poland.

[#]SDB and KP contributed equally as co-senior authors.

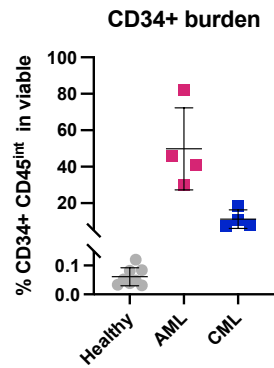
Correspondence:

K. PIWOCKA - k.piwocka@nencki.edu.pl

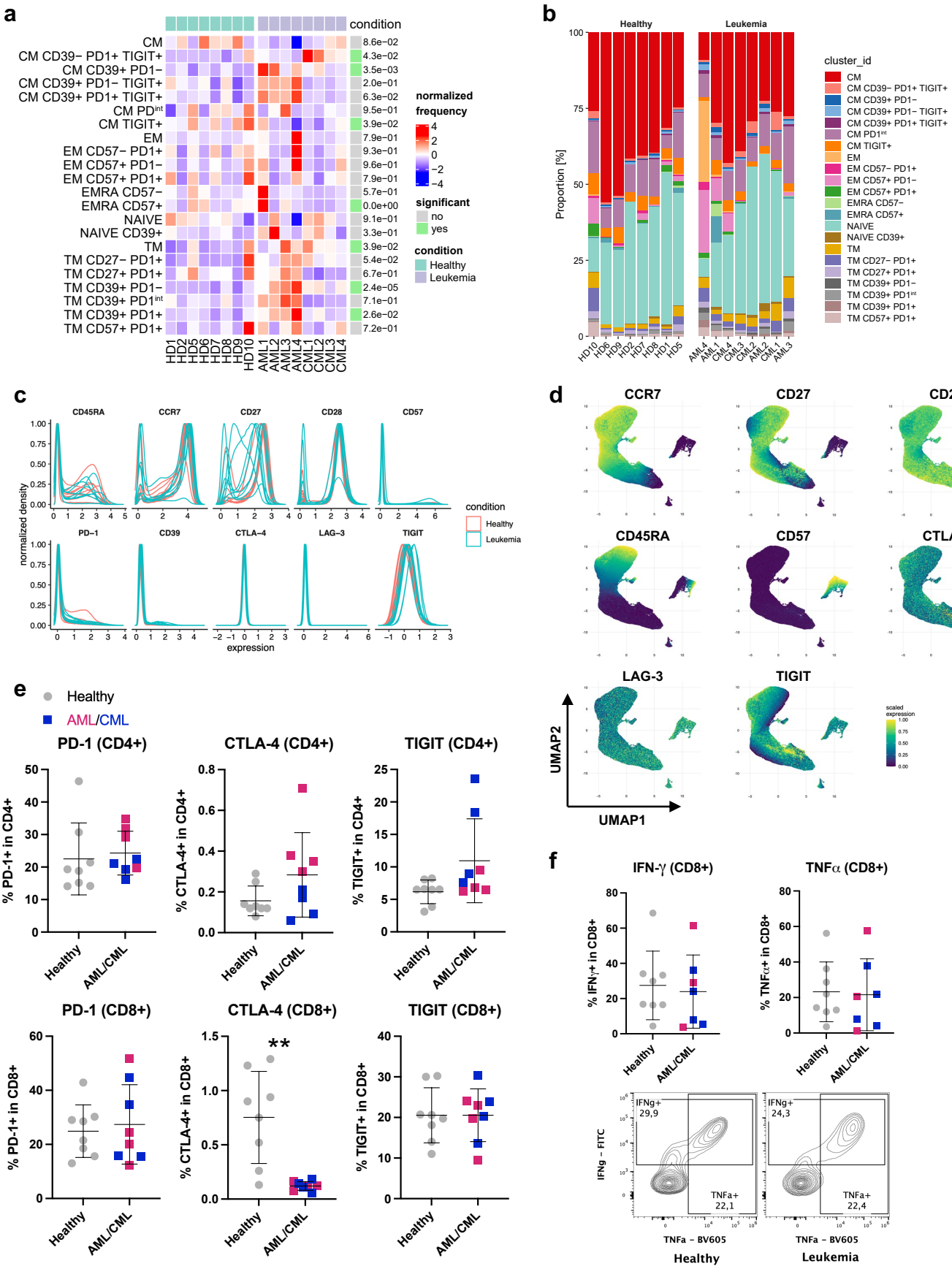
S. DE BIASI - debiasisara@yahoo.it

<https://doi.org/10.3324/haematol.2022.281713>

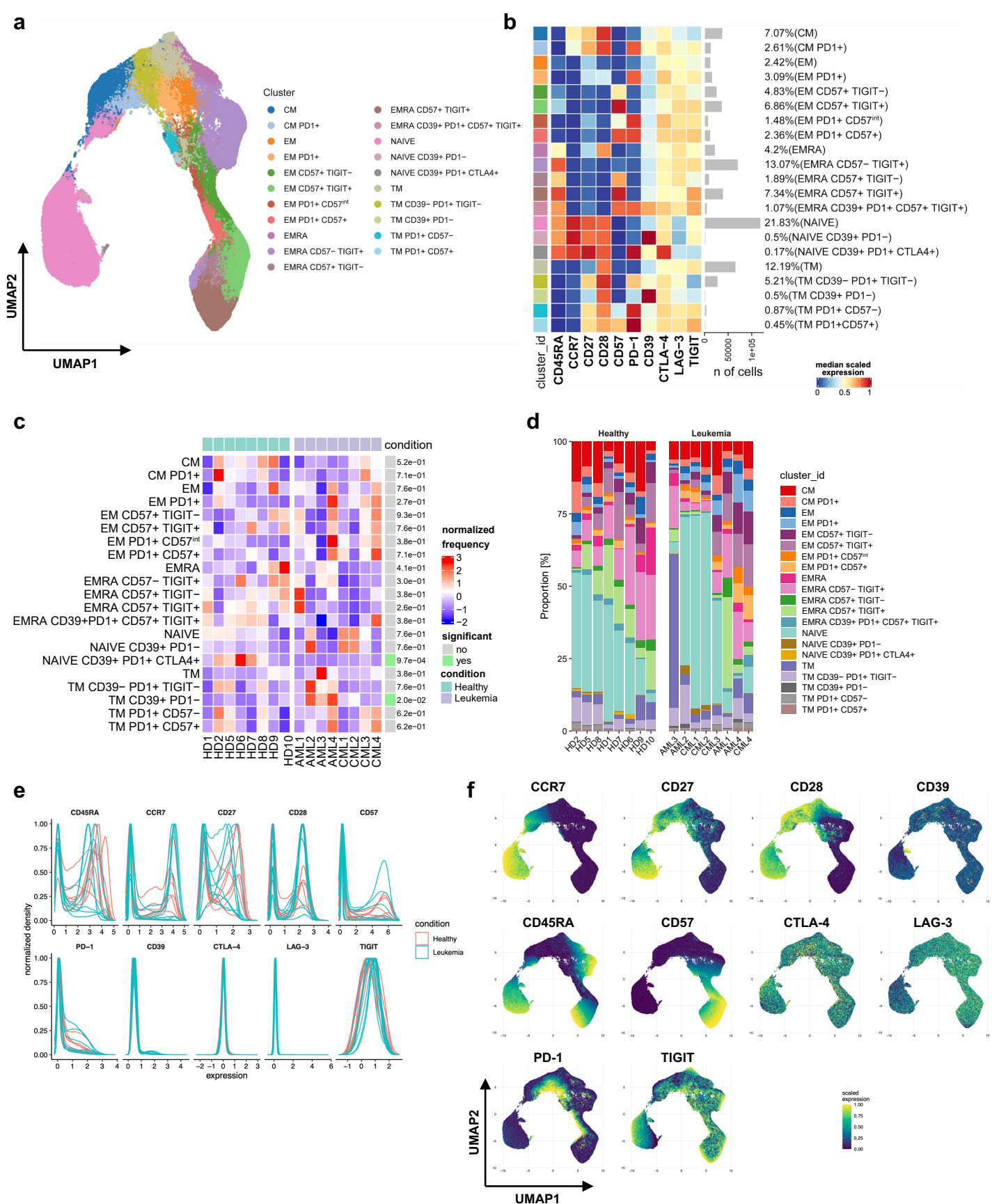
Patient	Sex	Age	Genetic background of leukemia					Mortality (days survived following diagnosis)	%CD34+ in PB	%CD38- in CD34+
			<i>FLT3-ITD</i>	<i>NPM1</i>	<i>BCR-ABL1</i>	<i>CBFB-MYH11</i>	<i>AML1-ETO</i>			
AML 1	M	73	not analysed					dead (27)	41,1	83,3
AML 2	F	24	---	---	---	---	---	alive	45,8	77,2
AML 3	M	69	---	---	---	---	---	dead (30)	30,2	88,8
AML 4	M	79	---	---	---	---	---	dead (132)	82,1	91,7
CML 1	F	43	---	---	+	---	---	alive	8,24	16,1
CML 2	F	34	---	---	+	---	---	alive	18,6	17,8
CML 3	F	54	---	---	+(b2a2)	---	---	alive	10,8	28,8
CML 4	F	72	---	---	+(b3a2)	---	---	alive	7,41	9,83



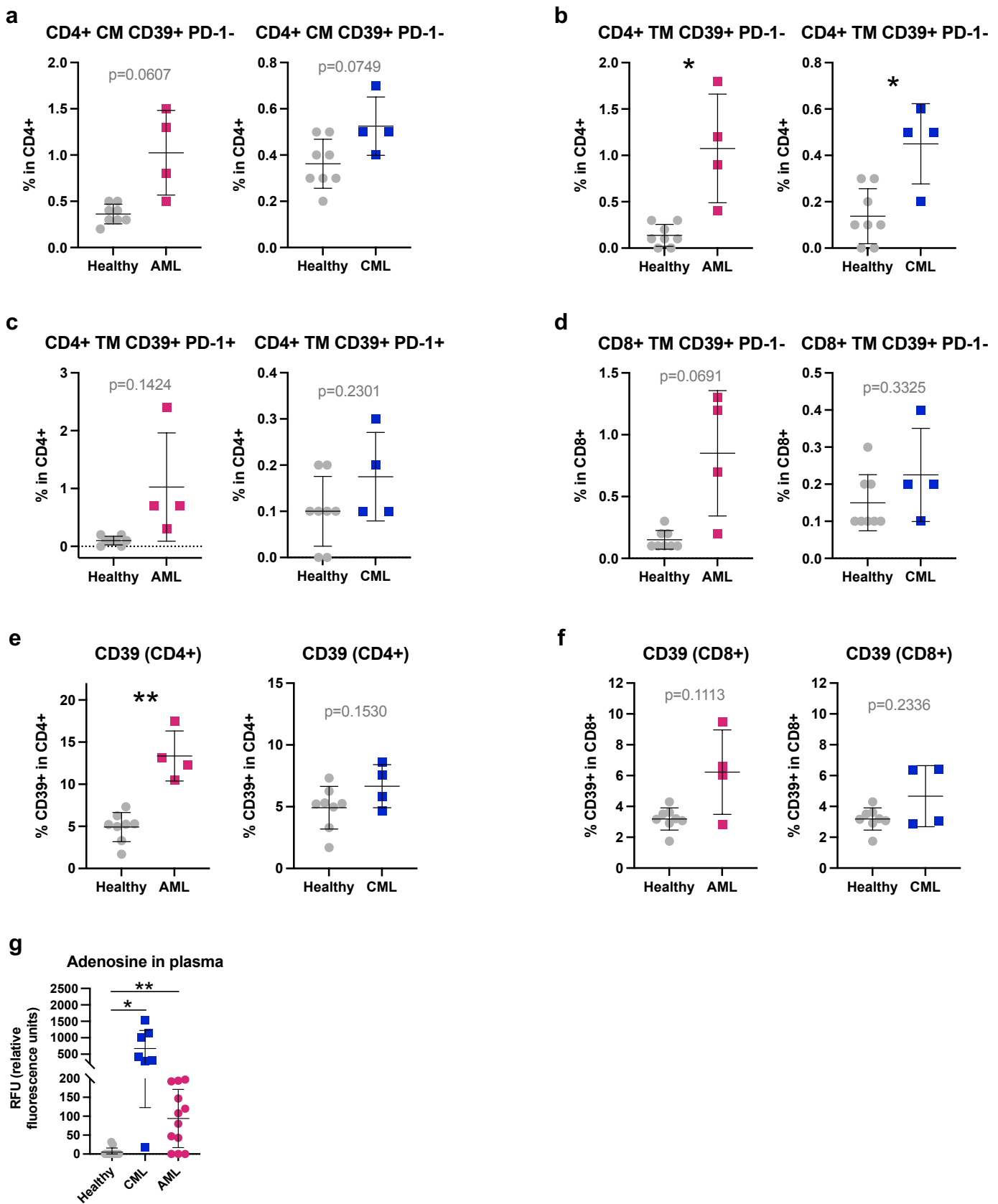
Supplementary Table 1. Clinical features and CD34+ leukemic cells burden in AML/CML patients used in the study. The table presents clinical features of AML and CML patients used for T cell phenotyping in the study – sex, age, mortality, data on CD34+ and CD38- leukemic cells in PB, as well as genetic background. All samples were collected at diagnosis. Patients were screened for most common mutations detected in AML and CML, without further sequencing. Initial diagnosis of AML/CML was performed based on bone marrow aspirate evaluation (by morphologic myelogram and phenotypic analysis of CD34+ cells by flow cytometry). AML was defined as $\geq 20\%$ blasts with myeloid morphology and phenotype, CML was further confirmed by detection of *BCR-ABL1* transcript. All CML patients were in chronic phase and untreated with any drugs at the moment of blood acquisition.



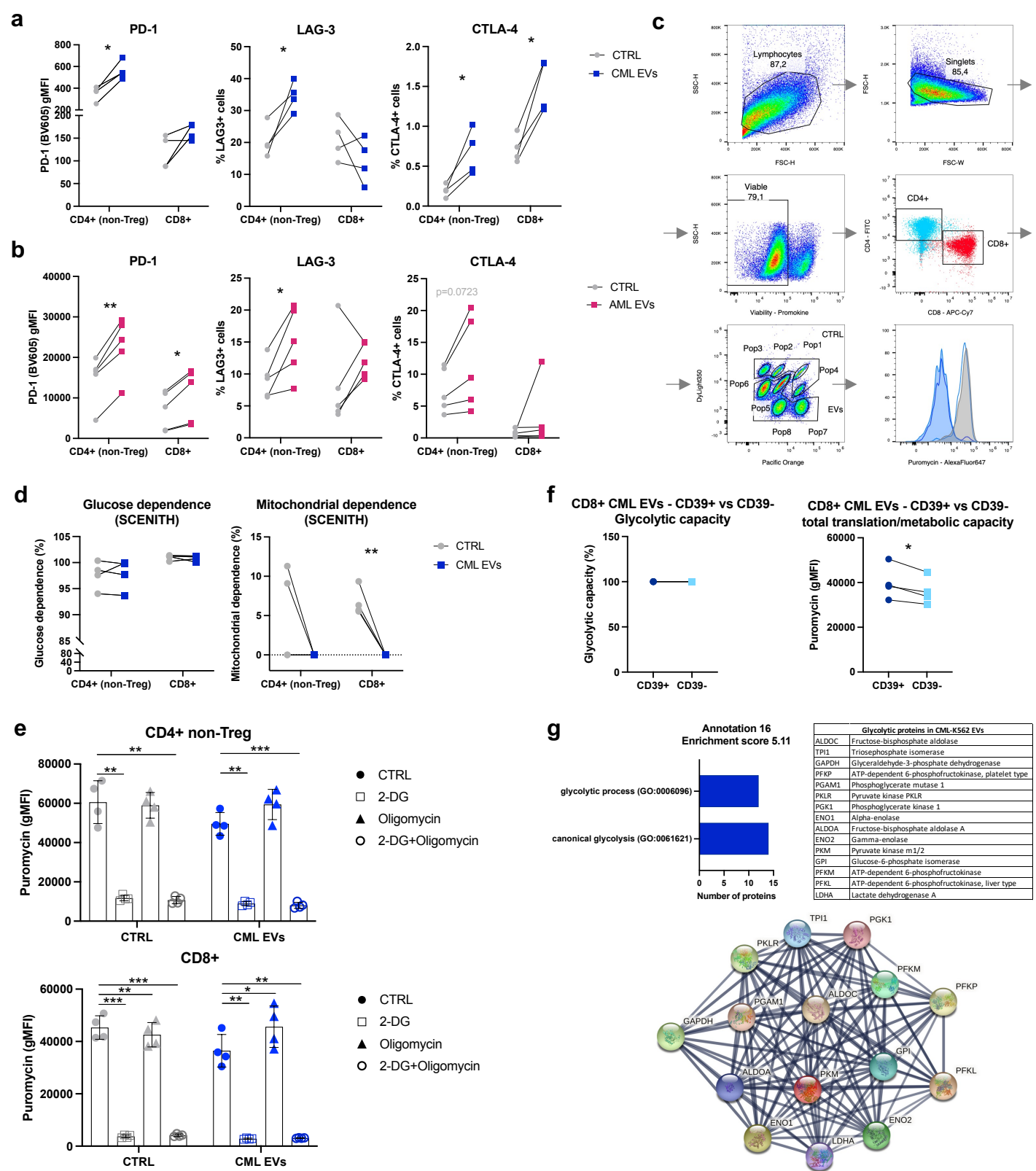
Supplementary Figure 1A. Unsupervised analysis of CD4⁺ T cells in AML/CML patients and healthy controls (in relation to main Figure 1A-C). (a) Differential analysis of healthy donors (n=8) and leukemic patients (n=8) samples. Heatmap colors represent relative cell frequencies, as indicated on the scale on the right, with red indicating overrepresentation and blue underrepresentation. Bars on the right indicate statistical significance (statistically significant differences in green) and adjusted p values are shown. (b) Distribution of cell clusters/subsets (identified in Figure 1A) in each single sample of healthy donors and leukemic patients used in the analysis. (c) Histogram overlays of phenotypic markers analyzed in each of the analyzed samples, as quality control of signal stability across samples and acquisition days. (d) UMAP graphs showing relative expression of CCR7, CD45RA, LAG-3, CD27, CD57, TIGIT, CD28, CTLA-4 on CD4⁺ T cells, clustered as shown in Figure 1A. (e) Expression of PD-1, CTLA-4 and TIGIT on CD4⁺ and CD8⁺ T cells (specified) in AML and CML patients and healthy donors. Mean ± SD is presented, unpaired t-test with Welch's correction (n=8 AML/CML patients (4 AML, 4 CML) and 8 healthy donors). (f) Abundance of CD8⁺ cytotoxic T cells expressing proinflammatory cytokines interferon- γ and TNF- α in AML and CML patients and healthy donors. Mean ± SD is presented, unpaired t-test with Welch's correction (n=7 AML/CML patients (3 AML, 4 CML) and 8 healthy donors). Representative plots are shown below.



Supplementary Figure 1B. Unsupervised analysis of CD8+ T cells in AML/CML patients and healthy controls. (a) Uniform Manifold Approximation and Projection (UMAP) representation of CD8+ T cells landscape. Different subsets and clusters (identified by FlowSOM) are indicated in unique colors assigned, as annotated. (b) Heatmap representation of CD8+ T cells landscape, with different subsets and clusters (unique colors annotated, as in UMAP in (a)), identified by FlowSOM. Percentage and name of each cluster in the analysis are shown next to the heatmap. Heatmap colors represent median expression of specified markers for each cluster, with blue as low and red as high expression. (c) Differential analysis of healthy donors (n=8) and leukemic patients (n=8) samples. Heatmap colors represent relative cell frequencies, as indicated on the scale on the right, with red indicating overrepresentation and blue underrepresentation. Bars on the right indicate statistical significance (statistically significant differences in green) and adjusted p values are shown. (d) Distribution of cell clusters/subsets (identified in (a)) in each single sample of healthy donors and leukemic patients used in the analysis. (e) Histogram overlays of phenotypic markers analyzed in each of the analyzed samples, as quality control of signal stability across samples and acquisition days. (f) UMAP graphs showing relative expression of CCR7, CD45RA, PD-1, CD27, CD57, TIGIT, CD28, CTLA-4, CD39, LAG-3 on CD8+ T cells, clustered as shown in (a) and (b).



Supplementary Figure 2A. CD39-expressing subsets and adenosine level in PB of patients, demonstrated separately for AML and CML patients (in relation to main Figure 1A-E). (a)-(d) Abundance of specified subsets of CD4+ and CD8+ T cells, as identified by unsupervised analyses, compared separately between healthy donors (n=8) and each AML (n=4) and CML (n=4) patients (in relation to Fig. 1C). Mean \pm SD is presented, unpaired t test with Welch's correction. (e)-(f) Expression of CD39 on CD4+ and CD8+ T cells, compared separately between healthy donors (n=8) and each AML (n=4) and CML (n=4) patients (in relation to Fig. 1D). Mean \pm SD is presented, unpaired t test with Welch's correction. (g) Adenosine level in plasma, compared separately between healthy donors (n=8) and each AML (n=12) and CML (n=7) patients (in relation to Fig. 1E). Data is shown as relative fluorescence units (RFU) in a fluorometric assay, following fluorescence subtraction of endogenous background samples. Mean \pm SD is presented, unpaired t test with Welch's correction. *p<0.05, **p<0.01.



Supplementary Figure 2B. Phenotypic and metabolic (SCENITH) analyses of CD4+ (non-Treg) and CD8+ T cells treated with leukemic extracellular vesicles. (a) Expression of PD-1, LAG-3 and CTLA-4 on CD4+ (non-Treg) and CD8+ T cells cultured with CML (K562-derived) EVs. Data are from 4 experiments (n=4). (b) Expression of PD-1, LAG-3 and CTLA-4 on CD4+ (non-Treg) and CD8+ T cells cultured with AML (MOLM-14-derived) EVs. Data are from 5 experiments (n=5). For (a) and (b), pairing was done for samples that were used to treat the same batch of (primary) T cells, two-tailed paired t-test. *p<0.05, **p<0.01. (c) Representative gating strategy for SCENITH analysis of T cells, following culture with leukemic EVs. T cells were first gated as viable either CD4+ or CD8+ T cells, followed by separation of differently treated samples based on DyLight350/Pacific Orange barcoding. Each population was then analyzed for amount of puromycin, indicative of translation efficiency and metabolic activity. (d) Glucose and mitochondrial dependence of CD4+ non-Treg and CD8+ T cells following treatment with leukemic EVs, as measured by SCENITH. (e) Translation intensity (corresponding to metabolic activity), measured by puromycin staining in CD4+ non-Treg and CD8+ T cells in control and leukemic EVs-treated cells, following treatment with 2-deoxyglucose (2-DG) and oligomycin in a SCENITH assay. Data points for control samples (without EVs) are shown in grey, for CML EVs in blue. (f) Glycolytic capacity and total translation (metabolic capacity) of CD8+ T cells treated with CML EVs, distinguished between CD39-expressing (CD39+) and CD39-negative (CD39-) T cells. For (d)-(f) data are from 4 experiments (n=4). Pairing was done for samples that were used to treat the same batch of (primary) T cells, two-tailed paired t-test. *p<0.05, **p<0.01, ***p<0.001. (g) Presence of glycolytic proteins in CML (K562-derived) EVs, detected in mass spectrometry analysis, re-analyzed from Swatler *et al.*, 2022, *Blood Advances* (data available in PRIDE repository, identifier PXD027240). Functional groups of glycolytic proteins (Annotation 16) were identified using David Bioinformatics Resources. Full list of proteins is shown in a table. As revealed by STRING analysis, glycolytic proteins shuttled in EVs constitute a functionally interconnected group of proteins.